A simple plume model induced by stack effect in a vertical shaft

Zhang Jingyan[1], Lu Weizhen[2], Huo Ran[3]
(1. Institute of Building Fire Research, China Academy of Building Research, Beijing 100013, China;
2. Department of Building and Construction, City University of Hong Kong, HKSAR, PRC;
3. State Key Laboratory of Fire Science, University of Science and Technology of China, Hefei 230026, China)

Abstract: After comparing the mechanism of tilted plume under stack effect with that of spill plume, the tilted plume model induced by stack effect in a vertical shaft is developed simply based on the theoretical results and a series of full-scale tests. It is shown that the two sides of plume are symmetrical and have an accordant regulation that the plume radius has a linear relation to the height z. The profile of fire plume under stack effect is similar to the windblown flame in wind tunnel, and the range of flame deflection angle is about from 50 to 60 degree.
Key words: stack effect; tilted plume profile; plume radius; flame deflection angle; air-entrainment

1 Introduction

When a mass of hot gases is surrounded by colder gases, the hotter and less dense mass will rise upward due to the density difference, or rather, due to buoyancy. This is what happens above a burning fuel source, and the buoyant flow, including any flames, is referred to as a fire plume. As the hot gases rise, cold air will be entrained into the plume, causing a layer of hot gases to be formed.

The buoyant axisymmetric plume [1], caused by a diffusion flame formed above the burning fuel, is the most commonly used plume in fire safety engineering. An axis of symmetry is assumed to exist along the vertical centerline of the plume, and air is entrained horizontally from all directions. Other fire plume categories include, for example, non-axisymmetric plumes, which allows air to be entrained from one side is more than the other side. The fire plume induced by stack effect belongs to this form.

The buoyant force causes an upward flow within the building shafts such as stairwells and elevator shafts if average indoor temperature is a few degrees higher than outdoor one. This is known as (normal) stack effect or chimney effect[2]. However, if the air is hot outside, a downward airflow occurs in an air-conditioned building, which is called reverse stack effect illustrated in Fig. 1. In sum, the reason that stack effect appears is the combined buoyancy- and pressure-driven flow generally[3]. So Stack effect induced a strong lateral air-entrainment. To the fire plume named tilted plume in this paper, this air-entrainment is forced. This flow is presented in Fig. 2.

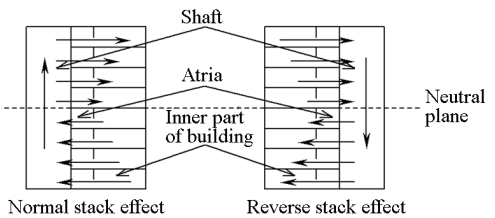

Fig. 1 Normal stack effect and reverse stack effect (Arrows indicate the direction of airflow)

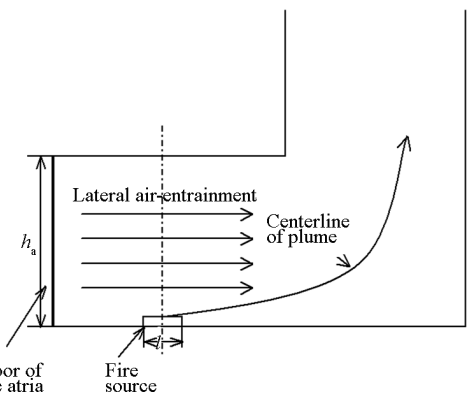

Fig. 2 A possible profile of plume under stack effect

Spill plume is another non-axisymmetric plume[4]. A typical spill plume is the flow from under a wide horizontal balcony over a vertical opening into an atmosphere without any restaint, e. g. no adherence to a vertical wall above the balcony and no allowance

Received 1 *July* 2008

for effects at the edges of the plume; it is a two-dimensional system. This flow is presented in Fig. 3.

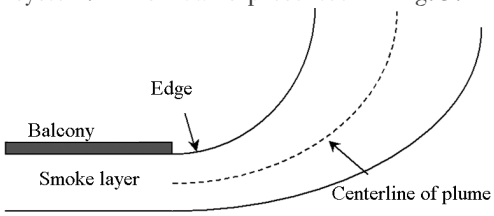

Fig. 3 Profile of balcony spill plume

Some physical scale and numerical models have been used to study on balcony plume[5]. The empirical equations which appeared in design guides such as NFPA 92B[6] were derived to estimate the air entrainment into the spill plume. A series of full-scale burning tests were performed at the PolyU/USTC Atrium constructed at the campus of the University of Science and Technology of China (USTC), Hefei, Anhui, China, as a collaboration project with The Hong Kong Polytechnic University (PolyU)[7]. Though the spill plume is similar to tilted plume in appearance, the mechanism between them is different. Spill plume appears due to the expansibility of smoke layer in upper space of fire room. Few people studied on the plume model induced by stack effect. So based on the ideal plume theory, a series of full-scale tests were performed for establishing the tilted plume model in this paper.

2 Theoretical background

In this section, we shall set up the fundamental equations for continuity, momentum, and buoyancy and thus arrive at analytical solutions for the equations of profile, mass flow, velocity, and temperature of the gases in this simplified plume.

2.1 Construction idea of the tilted plume model

We seek analytical expressions for the following variables as a function of height z:

The temperature difference at height z, $\Delta T(z)$ given in [K];

The radius of the plume at height z, $b(z)$ given in [m];

The upward gas velocity at height z, $u(z)$ given in [m/s];

The plume mass flow at height z, $\dot{m}_p(z)$ given in [kg/s].

An obvious difference between tilted plume and ideal plume is the air-entrainment. In tilted plume, considered as a two-dimension plume, the air-entrainment at the two sides of plume is unbalanced. The air-entrainment at the side of windward is more than the side of leeward. So the radius of the tilted plume can be produced from such model that a plume only under the effect of forced air-entrainment subtracts from a combined forced and natural air-entrainment plume. Fig. 4 shows the construction of tilted plume model.

To arrive at simple analytical solutions expressing the plume properties, we must make many restricting assumptions:

1) We assume that the boundary of windward is vertical and has no contribution to the profile of plume in Fig. 4(a) and Fig. 4(b) to simplify the solution;

2) We assume that there are no heat losses in the system due to radiative heat losses;

3) We assume that the natural air-entrainment at the edge of the plume is proportional to the local gas velocity in the plume, so that the entrainment velocity can be written as $v = \alpha u$, where α is a constant which need to be estimated in full-scale tests;

4) We assume that the entrainments are ignored except for the windward and leeward;

5) We assume that there are only small density differences with height.

2.2 Theoretical tilted plume model

We start by setting up general expression for the mass flow. The expression will then be incorporated in the differential equations for continuity of mass, and we will examine solutions to the differential equations. This will allow us, through dimensional analysis, to identify the constants arising from the assumed solutions to the differential equations and thereby set up expressions for the above mentioned variables.

2.2.1 The combined forced and natural air-entrainment plume in Fig. 4(a)

The expression for the mass flow rate at some height z, where the plume radius equals $r_1(z)$ and the cross-sectional area equals $r_1(z)l$, can be written as

$$\dot{m}_p = r_1(z)l\rho u(z) \tag{1}$$

where ρ is the density of fire plume and l is the diameter of fire source.

The differential buoyancy force acting on the mass within the small differential segment dz can be expressed as

$$dF = g(\rho_\infty - \rho) \cdot dz \cdot lr_1(z) \tag{2}$$

where g is the acceleration due to gravity. The time rate of momentum (mass flow times velocity) at height z can be written as

$$\dot{m}_p u(z) = lr_1(z)\rho u(z)^2 \tag{3}$$

These three equations will be used later to set up two differential equations, one for continuity and one for momentum and buoyancy.

Assuming that there are no radiative heat losses in the plume, the energy flow rate of the gases at height z can be written as

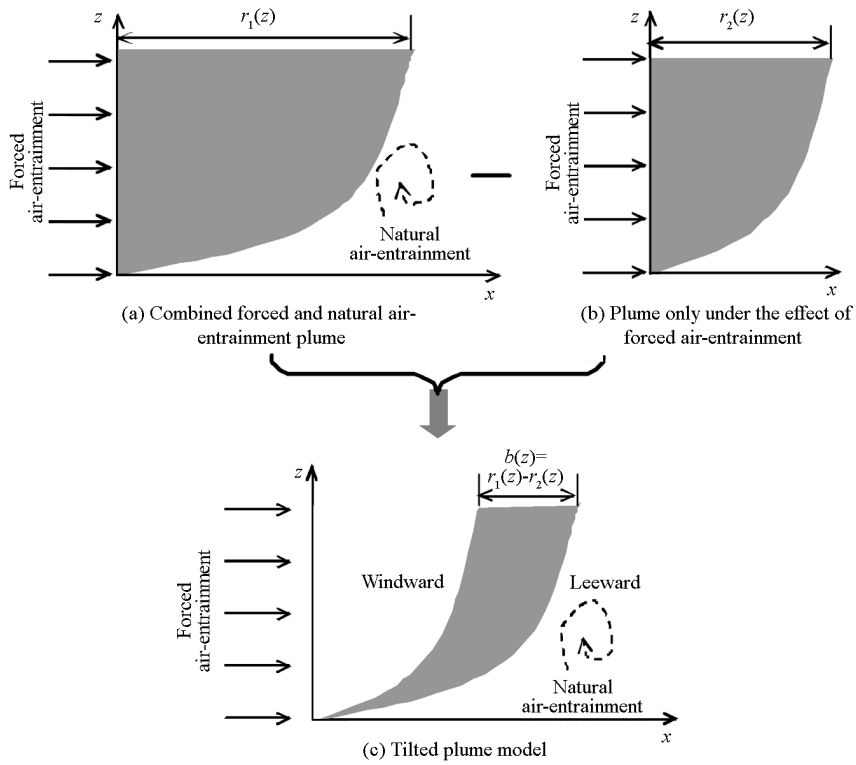

Fig. 4 The construction of titled plume model

$$\dot{Q} = \dot{m}_p c_p \Delta T = l r_1(z) \rho u(z) c_p \Delta T \quad (4)$$

where c_p is the specific heat capacity at constant pressure of the gases. Using the ideal gas law and rewriting the temperature difference as $\Delta T = (\Delta\rho/\rho) \cdot T_\infty$, the expression becomes

$$\dot{Q} = \dot{m}_p c_p \Delta T = l r_1(z) \rho u(z) c_p (\Delta\rho/\rho) \cdot T_\infty \quad (5)$$

We can therefore write the following relationship between density difference and energy release rate:

$$\Delta\rho = \frac{\dot{Q}}{l r_1(z) u(z) c_p T_\infty} \quad (6)$$

We now write the differential equations for mass and momentum/buoyancy with respect to height ($\frac{d}{dz}$). This will give us two differential equations. Assuming solutions for these and using dimensional analysis will give us the coefficients we need to arrive at analytical solutions for the variables we wish to express.

1) The continuity equation for mass

The continuity equation for mass simply states that the increase in mass flowing up through the differential element dz must be entrained through the sides of element dz. We shall first express the rate of change of mass flowing through the element and then express the mass entrained through the sides. Equating the two will lead to the differential equation that we seek.

The rate of change of mass over height dz can be written

$$\frac{d\dot{m}_p}{dz} = \frac{d(r_1(z) l \rho u(z))}{dz} \quad (7)$$

The rate at which air is entrained in through the sides of element dz equals the area of the sides ($= l \cdot dz$) times the horizontal entrainment velocity, v, times the density of the ambient air, ρ_∞. Earlier we assumed that the horizontal entrainment velocity could be expressed in terms of the upward velocity as $v = \alpha u$. In this model, an additional horizontal entrainment velocity, $v(z)$, need to be considered. To get the rates of entrained air per unit height we must also divide by dz, which give

$$l \cdot \alpha \cdot u(z) \cdot \rho \cdot dz/dz + l \cdot v(z) \cdot \rho \cdot dz/dz \quad (8)$$

Where $v(z)$ is adopted as the average velocity $\bar{v}$ for simplified solution.

We now Eq. (7) and Eq. (8), since the rate of change of mass over dz must equal the rate of mass entrained through the sides of dz, resulting in the continuity equation

$$\frac{d(r_1(z) u(z))}{dz} = \alpha u(z) + \bar{v} \quad (9)$$

2) The momentum and buoyancy equation

The rate of change of momentum over height dz must equal the buoyancy forces per unit height acting on the element dz. Differentiating Eq. (3) with respect to height, the rate of change of momentum per unit height z becomes

$$\frac{d\left[\dot{m}_p u(z)\right]}{dz} = \frac{d\left[lr_1(z)\rho u(z)^2\right]}{dz} \tag{10}$$

The differential buoyancy force acting on the mass within the small differential segment dz was given by Eq. (2). To get the buoyancy force acting on element dz per unit height, we divide Eq. (2) by dz, getting

$$dF/dz = g(\rho_\infty - \rho)\, lr_1(z) \tag{11}$$

Equating the rate of change of momentum with the buoyancy force per unit height, we get

$$\frac{d\left[lr_1(z)\rho u(z)^2\right]}{dz} = g(\rho_\infty - \rho) lr_1(z) \tag{12}$$

Again we make use of the weak plume assumption, so the ρ is assumed constant with height. Further, we wish to express the density difference, $\Delta\rho$, in terms of the energy release rate. Using Eq. (6) and treating ρ and π as constants, we arrive at the differential equation

$$\frac{d\left[lr_1(z)\rho u(z)^2\right]}{dz} = \frac{\dot{Q}g}{u(z)c_p T_\infty} \tag{13}$$

We will need to make one further assumption to arrive at an easily manageable differential equation for the momentum and buoyancy. We assume that ρ in the above equation is roughly equivalent to ρ_∞, which can be justified by the fact that we are considering the weak plume. Eq. (13) therefore becomes what we shall call the momentum-buoyancy equation

$$\frac{d\left[lr_1(z)\rho_\infty u(z)^2\right]}{dz} = \frac{\dot{Q}g}{u(z)c_p T_\infty} \tag{14}$$

The main results from the two last sections are two differential equations, the continuity Eq. (9) and the momentum-buoyancy Eq. (14).

3) Solution of the two differential equations

To facilitate an analytical solution of the Eq. (9) and Eq. (14), we shall assume that the radius, $r_1(z)$, and the velocity, $u(z)$, change as some power of the height, z, and write

$$\begin{aligned} r_1(z) &= c_1 z^m \\ u(z) &= c_2 z^n \end{aligned} \tag{15}$$

where c_1 and c_2 are all constants.

Eq. (9) becomes

$$\frac{d(c_1 c_2 z^{m+n})}{dz} = \alpha c_2 \dot{z}^n + \bar{v} \tag{16}$$

Similarly, Eq. (14) becomes

$$\frac{d(c_1 c_2^2 z^{m+2n})}{dz} = \frac{\dot{Q}g}{c_2 z^n l\rho_\infty c_p T_\infty} \tag{17}$$

The power of z must be the same on both sides of the Eq. (16) and Eq. (17) respectively. We can therefore get m, n:

$$\begin{aligned} m &= 1 \\ n &= 0 \end{aligned} \tag{18}$$

further,

$$\begin{cases} r_1(z) = c_1 z \\ u(z) = c_2 \\ c_1 c_2 = \alpha c_2 + \bar{v} \\ c_1 c_2^3 = \dot{Q}g/(l\rho_\infty c_p T_\infty) \end{cases} \Rightarrow$$

$$\begin{cases} r_1(z) = c_1 z \\ u(z) = c_2 \\ c_1 = \alpha + \bar{v}/\left[\sqrt[3]{D_1 + \sqrt{D_2}} + \sqrt[3]{D_1 - \sqrt{D_2}} - (\bar{v}/3\alpha)\right] \\ c_2 = \sqrt[3]{D_1 + \sqrt{D_2}} + \sqrt[3]{D_1 - \sqrt{D_2}} - (\bar{v}/3\alpha) \\ D_1 = \dfrac{c\dot{Q}}{2\alpha} - \dfrac{\bar{v}^3}{27\alpha^3} \\ D_2 = \left(\dfrac{c\dot{Q}}{2\alpha} - \dfrac{\bar{v}^3}{27\alpha^3}\right)^2 - \dfrac{\bar{v}^6}{729\alpha^6} \\ c = g/(l\rho_\infty c_p T_\infty) \end{cases} \tag{19}$$

In Eq. (19), $u(z)$ is calculated to be a constant c_2. Factually, the vertical velocity of flame is decreased with the height z due to the air-entrainment. The reason perhaps is that the situation is idealized excessively. So the actual measurement c_2 is regarded as the maximum velocity in the vertical of flame in this paper.

2.2.2 The plume only under the effect of forced air-entrainment in Fig. 4(b)

This tilted plume is similar to the windblown flames in wind tunnel ostensibly. The main effect of wind is to bend or deflect the flames away from the vertical. Another effect, observed in wind tunnel studies by Welker and Sliepcevich[8] is "flame trailing," in which the flames trail off the burner along the floor in the downwind direction for a significant distance. Flame trailing was thought to be associated primarily with fuel vapors of greater density (higher molecular weight) than air, as was the case with all the various liquid fuels used in the experiments.

Wind tunnel measurements of flame deflection angle, involving fire diameters in the range 0.10 ~ 0.60 m, and large scale data for square LNG pools in the effective diameter range 2 ~ 28 m, obtained by Attalah and Raj, have been found to correlate well against the ratio of wind velocity to the maximum velocity in the flame according to Eq. (20)[9,10]. The relationship indicates that a flame deflection angle of approximately 25° can be expected for a velocity ratio of 0.10.

Effects of wind on flame length were minor for velocity ratios up to 0.35 (flame deflection angle of approximately 60°). Data by Huffman et al.[11] indicate that at the considerably higher velocity ratio of 1.0, flame lengths are approximately 30 % greater than under quiescent conditions.

So the two sides of plume are symmetrical and have accordant regulation. And the profile of plume induced by stack effect can be described as Fig. 5.

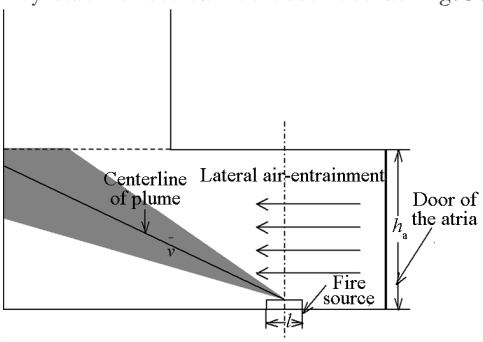

Fig. 5 Sketch map of plume profile induced by stack effect through theoretical analysis

Further, for estimating the tilted plume model under stack effect, a direct project is full-scale test to compare.

3 Apparatus and experimental procedure

The experiments were performed at the PolyU/USTC Atrium, which provides a 2 m × 2 m × 15 m high shaft and a 2 m × 4 m × 3 m high atria for the full-scale tests. Fig. 6 and Fig. 7 show the photographs and sketch of equipment. A thermography was used to record the temperature field and the profile of fire plume. The velocity at inlet was measured, whose average would be used in theoretical analysis. During the tests, four kinds of fire source are considered: l = 0.5, 0.6, 0.7, 0.8 m. The fuel is gasoline. Temperature of environment is 278 K.

(a) Shaft (b) Whole device

Fig. 6 Photographs of the shaft and the whole device

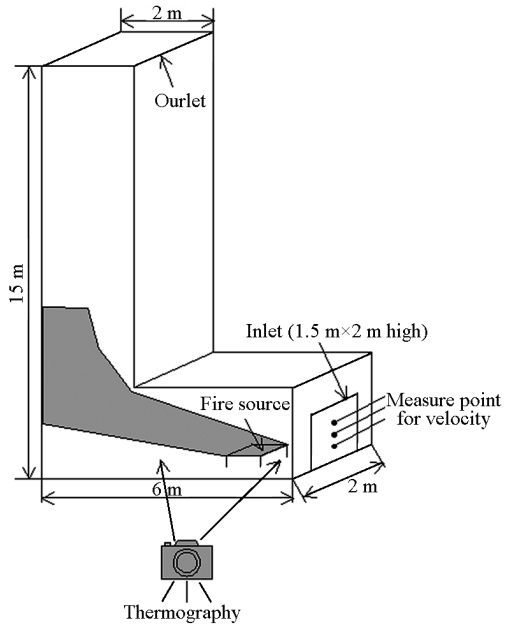

Fig. 7 Sketch map of the equipment

4 Analysis of the results

Some pictures were selected from the thermography data, which are shown in Fig. 8. And the angles that windward of fire plume tilts (θ) were measured.

From Fig. 8, we can find the angles that windward of fire plume tilts have no obvious regularity to the character of fire source. With the increase of fire source dimension, the buoyancy is increased. At the same time, the average of velocity at inlet ($\bar{v}$) is enhanced due to the raised temperature in the shaft. So the proportion of vertical velocity to horizontal velocity (tg θ) can't be educed simply. The range of the angle is about 50° to 60° under the different heat release rate.

5 Discussion and conclusions

Many applications in fire safety engineering have to do with estimating the properties of fire plume such as radius, maximum velocity, maximum temperature, and so on. This depends directly on how much mass and energy is transported to the plume. In this paper, based on the theoretical results and full-scale tests, a simple plume model induced by stack effect in a vertical shaft is developed. The two sides of plume are symmetrical and have accordant regulation, where r_1 and r_2 have linear relations to the height z. After comparing with wind tunnel, it is shown that the profile of fire plume under stack effect is similar to the windblown flame in wind tunnel, and the range of flame deflection

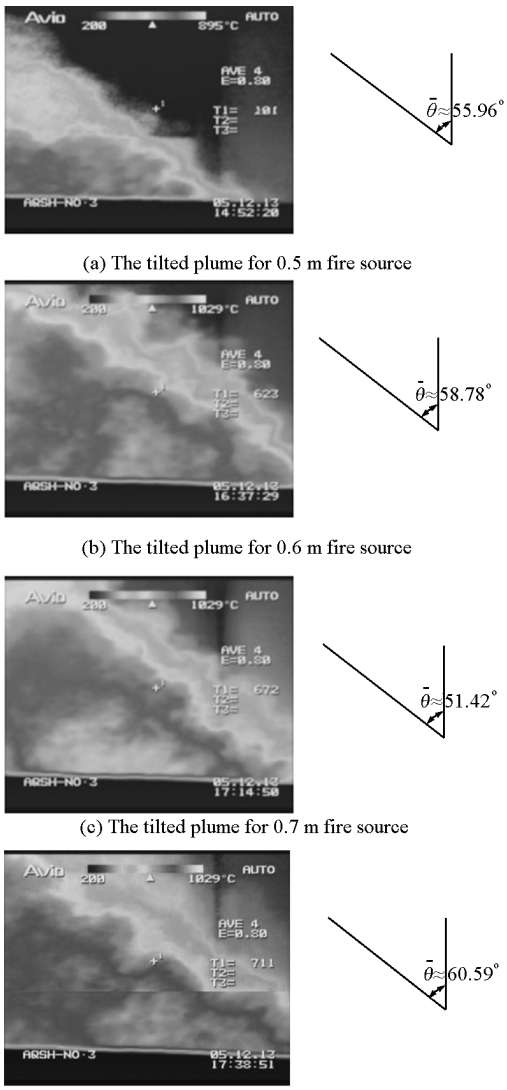

(a) The tilted plume for 0.5 m fire source

(b) The tilted plume for 0.6 m fire source

(c) The tilted plume for 0.7 m fire source

(d) The tilted plume for 0.8 m fire source

Fig. 8 The tilted plume for different fire sources

angle is about from 50°to 60°.

The air-entrainment coefficient α is an important factor. From Eq. (19), it is found that the radius and the maximum velocity depend on α deeply. The air-entrainment coefficient is perhaps different from that in free plume. And its value needs to be measured especially in the further work.

Acknowledgements

The paper was partially supported by the National Key Project of Scientific and Technical Supporting Programs Funded by Ministry of Science & Technology of China (Grant No: 2006BAJ13B03) and the RGC CERG Grant # CityU1253/04E from Hong Kong Research Grant Council, HKSAR.

References

[1] Heskestad G. Fire plumes[A], SFPE Handbook of Fire Protection Engineering (2nd ed.)[C]. Quincy: National Fire Protection Association, 1995.

[2] Klote J H. A general routine for analysis of stack effect[A]. NISTNR 4588[C]. National Institute of Standards and Technology. Gaithersburg, Md: 1991.

[3] Cooper L Y. Calculation combined buoyancy-and pressure-driven flow through a shallow, horizontal, circular vent: application to a problem of steady burning in a ceiling-vented enclosure[J]. Fire Safety Journal, 1996, 27: 23 – 35.

[4] Thomas P H, Morgan H P, Marshall N. The spill plume in smoke control design[J]. Fire Safety Journal, 1998, 30: 21-46.

[5] Chow W K. Numerical simulations on balcony spill plume[J]. Fire and Materials, 1999, 23: 91-99.

[6] NFPA 92B Guide for Smoke Management Systems in Malls Atria, and Large Areas[S]. USA: National Fire Protection Association (NFPA). 1995.

[7] Chow W K, Fan Weicheng. The PolyU/USTC atrium, information leaflet[R]. Hong Kong: The Hong Kong Polytechnic University, 1998.

[8] Welker J R, Sliepcevich C M. Technical Report No. 2[R]. NBS Contract XST 1142 with University of Oklahoma, 1965.

[9] Attalah S, Raj P K. Interim report on phase II work, project IS-3. 1 LNG safety program[R]. American Gas Association, Arlington, VA, 1974.

[10] Heskestad G. Dynamics of the fire plume[J]. Roy. Soc. Lond. A, 1998, 356: 2815-2833.

[11] Huffman K G, Welker J R, Sliepcevich C M. Technical Report No. 1441-3[R]. NBS Contract CST 1142 with University of Oklahoma, 1967.

Author

Zhang Jingyan, male, was born in 1978. He graduated from USTC and now is a senior engineer at China Academy of Building Research, Beijing, China. Mr. Zhang has published over 20 papers. His current research is building fire research and fire risk evaluation etc. He can be reached by E-mail: cabrzjy@163.com